Available online at www.sciencedirect.com
ScienceDirect
J. Crystal Growth 00 (2014) 1–11
Journal Logo

Growth and doping of semipolar GaN grown on patterned sapphire substrates

F. Scholz [1a], T. Meisch[a], M. Caliebe[a], S. Schörner[a,b], K. Thonke[b], L. Kirste[c], S. Bauer[d], S. Lazarev[d], T. Baumbach[d]

[a] *Institute of Optoelectronics, Ulm University, 89069 Ulm, Germany*
[b] *Institute of Quantum Matter, Ulm University, 89069 Ulm, Germany*
[c] *Fraunhofer Institute of Applied Solid State Physics, Tullastrasse 72, 79108 Freiburg, Germany*
[d] *Synchrotron Facility at ANKA, KIT Karlsruhe, 76344 Eggenstein-Leopoldshafen, Germany*

Abstract

In order to achieve large area semipolar GaN layers with high crystal quality, we have etched trenches into n-plane and r-plane sapphire wafers exposing c-plane-like side-walls, from which GaN stripes can be grown by metalorganic vapor phase epitaxy mainly in c-direction, forming semipolar $\{10\bar{1}1\}$ or $\{11\bar{2}2\}$ surfaces after coalescence. Here, we describe how to improve such layers by optimizing the side-facet orientation and by including a SiN nanomask interlayer *in-situ* into the growth process, eventually resulting in a basal plane stacking fault density below $5{\cdot}10^3\,\mathrm{cm}^{-1}$. Moreover, doping experiments have revealed a substantially lower Mg incorporation efficiency on the $\{11\bar{2}2\}$ surface as compared to the c-plane, whereas Si does not show such differences.

Keywords: A1: Doping, A3: Metalorganic Vapor Phase Epitaxy, B1: Nitrides, B2: Semiconducting III-V materials

1. Introduction

Green light emitting diodes based on group-III nitrides still suffer from fairly low performance as compared to shorter wavelength blue emitters. One possible reason is the lattice mismatch induced strain of the GaInN quantum wells in the active region in such devices having a comparably large In content. This causes the formation of huge piezoelectric fields within the GaInN quantum wells separating electrons and holes spatially and hence reducing their recombination probability. By changing the main epitaxial growth direction from the conventional polar c-direction into less polar crystal directions, the internal fields can be strongly reduced. This approach is currently mainly investigated by growing on semipolar GaN wafers cut from thick c-plane material grown by other methods like hydride vapour phase epitaxy [1] or ammonothermal crystal growth [2, 3]. However, owing to the limited thickness of those c-plane wafers, semipolar bulk substrates cut from them are limited in size to a few square millimetres. On the other hand, approaches to grow semipolar GaN on flat foreign substrates of accurate orientation other than c-plane typically result in highly defective layers (see [4] and references therein). Obviously, growth in the polar c-direction leads to lowest defect densities. Therefore, we currently study a heteroepitaxial approach where the epitaxial process starts from c-plane-like sidewalls of trenches etched into sapphire wafers. The stripes nucleating on these side facets later coalesce to a closed surface with semipolar orientation. This technique was first proposed by Honda *et al.* to grow semipolar GaN planes on Si [5] and later applied to various directions of GaN by Okada *et al.* (see [6, 7, 8] and

[1] Corresponding author; Tel: +49-731-50-26052, Fax: +49-731-50-26049, e-mail: ferdinand.scholz@uni-ulm.de

Table 1. Semipolar GaN planes and respective sapphire surface orientations when growing out of trenches with c-plane like side facets.

Semipolar GaN top plane	Angle to *c*-plane	Required substrate surface facet	Angle between sidewall facet and surface
$\{11\bar{2}2\}$	58.4°	$\{10\bar{1}2\}$ *r*-plane	57.6°
$\{10\bar{1}1\}$	61.9°	$\{11\bar{2}3\}$ *n*-plane	61.2°

references therein). This procedure can be easily applied to large size sapphire wafers. Even first light emitting device structures have been successfully grown on such layers [9].

In this contribution, we describe how to optimize such large area semipolar GaN layers grown by metalorganic vapour phase epitaxy by applying similar strategies as have been successfully developed for planar c-plane layers. In particular, we have studied the applicability of a defect-blocking SiN nanomask layer [10, 11, 12] to our approach. Moreover, we have investigated the Si and Mg incorporation for achieving n- and p-type doping on these surfaces.

2. Experimental

All samples investigated in these studies have been grown by metalorganic vapor phase epitaxy (MOVPE) carried out in a commercial horizontal flow Aixtron-200/4 RF-HT reactor using the standard precursors trimethylgallium (TMGa), trimethylaluminum (TMAl), and ammonia (NH_3). In order to achieve $\{10\bar{1}1\}$ and $\{11\bar{2}2\}$ semipolar GaN surfaces, we used $\{11\bar{2}3\}$ (n-plane) and $\{1\bar{1}02\}$ (r-plane) sapphire wafers, respectively. The c-plane in these wafers is inclined by approximately 60 ° with respect to the surface, which is – as required – about the same angle as between the above mentioned GaN surfaces and the GaN c-plane (see Tab. 1). Periodically aligned grooves (about 3 μm wide / 6 μm period) along the in-plane m- and a-direction, respectively, have been etched by reactive ion etching (RIE) using BCl_3 as reactive gas after optical lithography. These grooves had a typical depth of about 1 μm with a c-plane-like sidewall on one side (Fig. 1, more details see below). In particular for the structures on n-plane sapphire, we covered all open areas except the c-plane-like side facet of the grooves (see Fig. 1) by another SiO_2 layer by directed sputtering after removing the remaining metal mask in order to suppress any unwanted nucleation in the subsequent growth process.

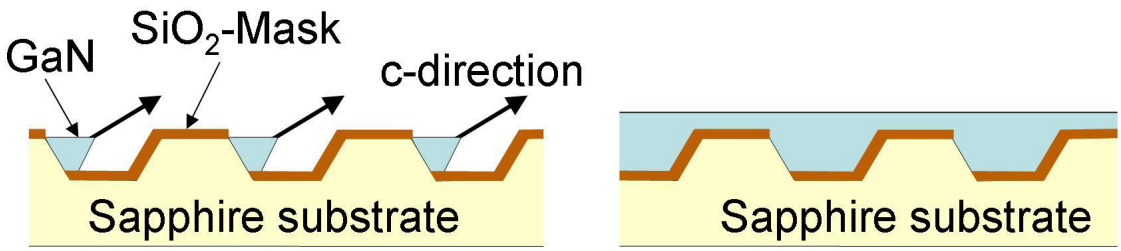

Figure 1. GaN growth nucleating at the inclined *c*-plane-like sidewalls of grooves etched into a foreign substrate (schematically). The growth first proceeds in *c*-direction (left), later the single stripes coalesce by lateral growth eventually forming a semipolar surface (right).

After the RIE etching, the MOVPE growth of several μm thick GaN layers was initiated with our standard oxygen doped low temperature AlN nucleation layer [13, 14]. By stopping the Ga flow after about 1.2 μm growth and opening the SiH_4 gas channel similarly as descibed in [12], we deposited a thin SiN nanomask interlayer in some samples before continuing the GaN layer growth. GaN doping studies have been performed using the standard precursors SiH_4 (100 ppm diluted in N_2) and Cp_2Mg, respectively.

All samples have been investigated by standard procedures including high-resolution X-ray diffraction (HRXRD) and low-temperature photoluminescence. For some of the samples, HRXRD measurements of diffuse intensity in

Table 2. Obtained surface roughness by varying the tilting angle during dry etching.

Wafer inclination during dry etching	RMS Roughness by AFM
0°	220 nm
6°	100 nm
8°	70 nm
10°	60 nm

three-dimensional reciprocal space were performed at the SCD beam-line at synchrotron ANKA of the KIT in Karlsruhe, Germany. The setup used to carry out the experiment, consisting of a six circles diffractometer and a linear detector (microstrip solid-state detector Mythen 1K), has been described in detail in our previous work [15, 16]. The basal plane stacking fault (BSF) density was determined accurately from the intensity profiles along the stacking fault streaks derived from three-dimensional reciprocal space maps [17].

3. Optimization of GaN growth

3.1. Trench side facet angle

When using our standard RIE process with a Ni-Au metal mask, the typical sidewall angles of our trenches etched into the r-plane sapphire wafers were about 65 ° to 70 °, i. e. they do not perfectly expose the inclined c-plane of the wafers (see Tab. 1). Unfortunately, we were not able to decrease this angle significantly by varying the dry-etching conditions. To achieve this goal anyway, we have mounted some r-plane sapphire wafers into our RIE reactor with a dedicated off-angle (see Tab. 2). This indeed helped to get the etched side-facet much closer to the c-plane facet of these sapphire wafers (Fig. 2). Moreover, we observed a systematic decrease of the RMS roughness of our $\{11\bar{2}2\}$ sample surfaces from about 200 nm (measured by AFM on $70\,\mu\text{m} \times 70\,\mu\text{m}$ areas on the exactly mounted reference sample) down to 60 nm for the 10 ° samples (see Tab. 2 and Fig. 3). Although the roughness data in this particular growth series are unexpectedly large, the observed trend seems to be significant. However, we did not see a significant change of other quality features like, e.g., the line width of our XRD rocking curves, which typically remained below 200 arcsec in all cases.

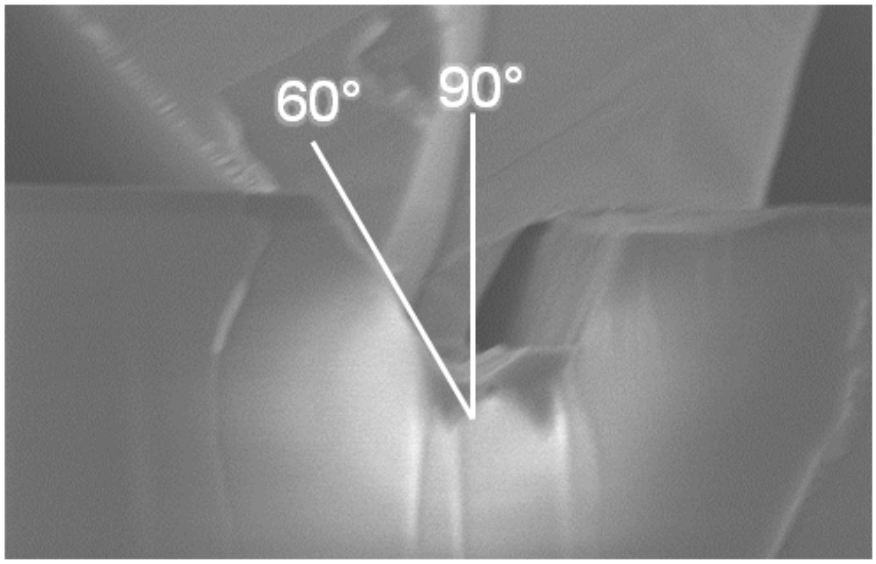

Figure 2. Trench etched after tilting the sample in the dry-etching chamber by 10 °. A facet angle of 60 ° was obtained.

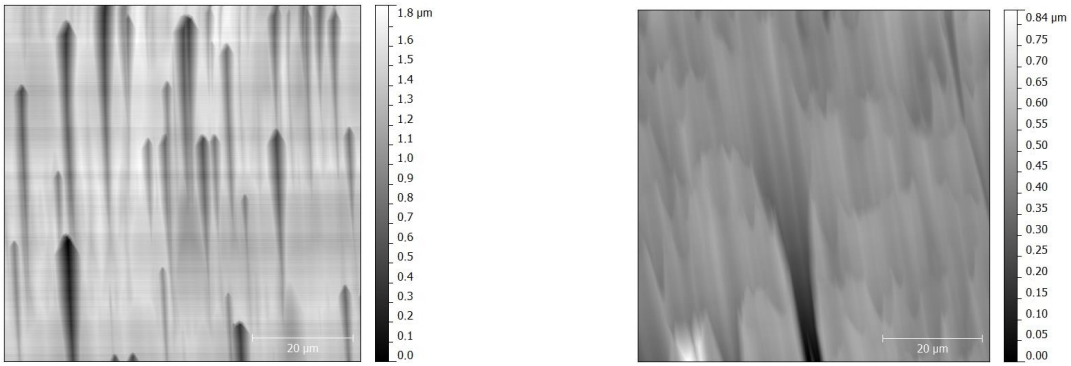

Figure 3. AFM measurements of two samples dry-etched with Ni-Au mask and different inclination angle in the RIE reactor of 0 ° (left) and 10 ° (right), c.f. Tab. 2.

Table 3. Obtained facet miscut and surface roughness by varying the pressure during our optimized dry etching process.

RIE pressure	Facet inclination	RMS Roughness by AFM
1.3 Pa	70°	60 nm
5.3 Pa	60°	10 nm

These findings motivated us to develop a new dry etching process which provides less steep side walls. Here, a negative photoresist is directly used as mask for the subsequent RIE process. The cross-linked photoresist stripes with a height of about 700 nm serve as a comparably stable mask. Now, the pressure of the RIE reactor influences the etching behavior strongly. At low pressure, the mechanical etching dominates, the resist keeps stable and trenches with steep side walls are achievable. Increasing the pressure, the chemical behavior of the etching process starts to dominate. The photoresist gets etched more laterally, leading to trenches with comparably flat side walls. Hence, it was possible to decrease the angle of the trench side walls by varying the RIE pressure, and we observed again a strong correlation between this angle and the surface quality of the subsequently grown GaN (Tab. 3 and Fig. 4). By increasing the pressure to 5.3 Pa, the angle could be reduced to 60°, very close to the c-plane facet in the $\{10\bar{1}2\}$ oriented sapphire substrate (58°), resulting in an RMS value of less than 10 nm. Under both conditions, a trench depth of about 360 nm was obtained.

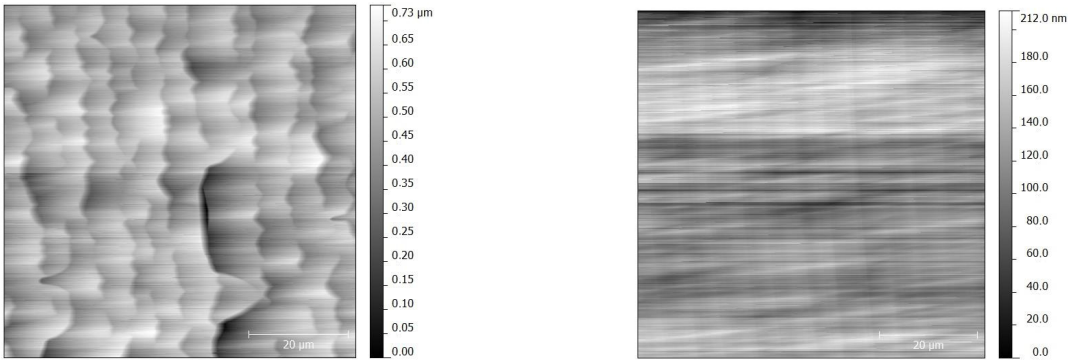

Figure 4. AFM measurements on two samples etched with photoresist mask under different RIE reactor pressure of 1.3 hPa (left) and 5.3 hPa (right), c.f. Tab. 3.

Table 4. Description of samples with and without SiN nanomask interlayer, as depicted in Fig. 6.

Sample ID	Type of sample	SiN interlayer	BSF density (cm^{-1})
S1	$\{10\bar{1}1\}$	no	$2.3 \cdot 10^4$
S2	$\{10\bar{1}1\}$	yes	$1.1 \cdot 10^4$
S3	$\{11\bar{2}2\}$	no	$7.9 \cdot 10^3$
S4	$\{11\bar{2}2\}$	yes	$4.4 \cdot 10^3$

3.2. SiN interlayer

For GaN growth on c-plane sapphire, typically a huge threading dislocation density of mid $10^9\,cm^{-2}$ is observed. One simple procedure to decrease this density by about one order of magnitude is the integration of a SiN nanomask layer [10, 11, 12]. Therefore, we have adopted this procedure here:

After 10 min GaN growth, at a distance of approximately 1.2 μm from the c-facet, GaN growth is interrupted for the *in-situ* deposition of a less than a monolayer thick SiN_x interlayer at the GaN growth temperature using SiH_4 and NH_3 as precursors for 3 min. Then, the GaN growth is continued. More details about this procedure can be found in [18]. Although this process is not yet optimized, we observed a significant improvement of our layers. In low temperature photoluminescence (Fig. 5), the defect-related peaks at energies below the dominant donor-bound excitonic peak at about 3.475 eV could be decreased. This is in particular true for the signals between 3.3 and 3.42 eV, which are assigned to stacking faults (SF), very common defects in semipolar GaN layers. In other reports, these SF peaks typically dominate the photoluminescence (PL) spectra (see, e.g., Ref. [19]) indicating significantly larger SF densities. Commonly reported densities are in the $10^5\,cm^{-1}$ range (see e.g. Ref. [20]). Only by applying a more complicated 2-step epitaxial lateral overgrowth procedure, Zhu *et al.* obtained similarly low SF PL peak intensities in such semipolar layers [21] without quantifying their values further.

This suppression of SFs may be a consequence of a better lateral overgrowth of the -c-wing of our initial stripes by the +c-wing of the neighbouring stripe, when the SiN interlayer is present, similar as observed by Zhu *et al.* [21]. Earlier studies have shown that most of the stacking faults are generated in the -c-wing [22].

The reduction of the SF densities could be further quantified by X-ray diffraction studies of the intensity distribution along stacking fault streaks (Fig. 6, for details of this method see Ref. [17]). On our $\{11\bar{2}2\}$ surface samples with a SiN nanomask inter-layer, an extremely low SF density below $5{\cdot}10^3\,cm^{-1}$ could be evaluated (Tab. 4). This value may be compared to commonly reported densities in the $10^5\,cm^{-1}$ range (see e.g. Ref. [20]).

4. Si and Mg doping

In order to eventually realize electroluminescence test structures, we have done investigations about n-type and p-type doping of our semipolar $\{11\bar{2}2\}$ GaN layers. To this end, we have grown GaN doped with Si and Mg, respectively, on semipolar templates which have been grown as described above. For comparison, just a half semipolar template wafer was put into the MOVPE reactor side by side with a half c-plane template wafer. Hence, both templates have been overgrown under identical conditions. The dopant precursor flows were varied between 5 and 15 sccm and between 125 and 425 sccm for the SiH_4 flow and the H_2 carrier gas flow through the Cp_2Mg bubbler, respectively. These samples have been analyzed by secondary ion mass spectrometry in order to determine their dopant profiles.

Indeed, we found an identical Si incorporation efficiency for both types of surfaces within this doping series (Fig. 7). Moreover, Hall experiments revealed good agreement between the Si concentration and the carrier concentration with slightly higher values for the latter, probably due to a fairly high background carrier concentration in the nominally undoped buffer layers. It may be noticed that our background carrier concentrations in nominally undoped c-plane layers are below $10^{17}\,cm^{-3}$. In our undoped semipolar layers, we found larger values, although such data are difficult to be quantified owing to their striped buffer structure and the integrated SiN nanomask layer.

However, the Mg incorporation into the $\{11\bar{2}2\}$ layers was strongly reduced as compared to the c-plane reference samples (Fig. 8). A similar reduction of the incorporation efficiency has been found earlier by Cruz *et al.* in layers using semipolar bulk templates cut from thick HVPE-grown c-plane wafers [23]. Although it is expected that the incorporation of Mg as a metal is mass-transport limited [23], this is obviously not the case on $\{11\bar{2}2\}$ facets, probably

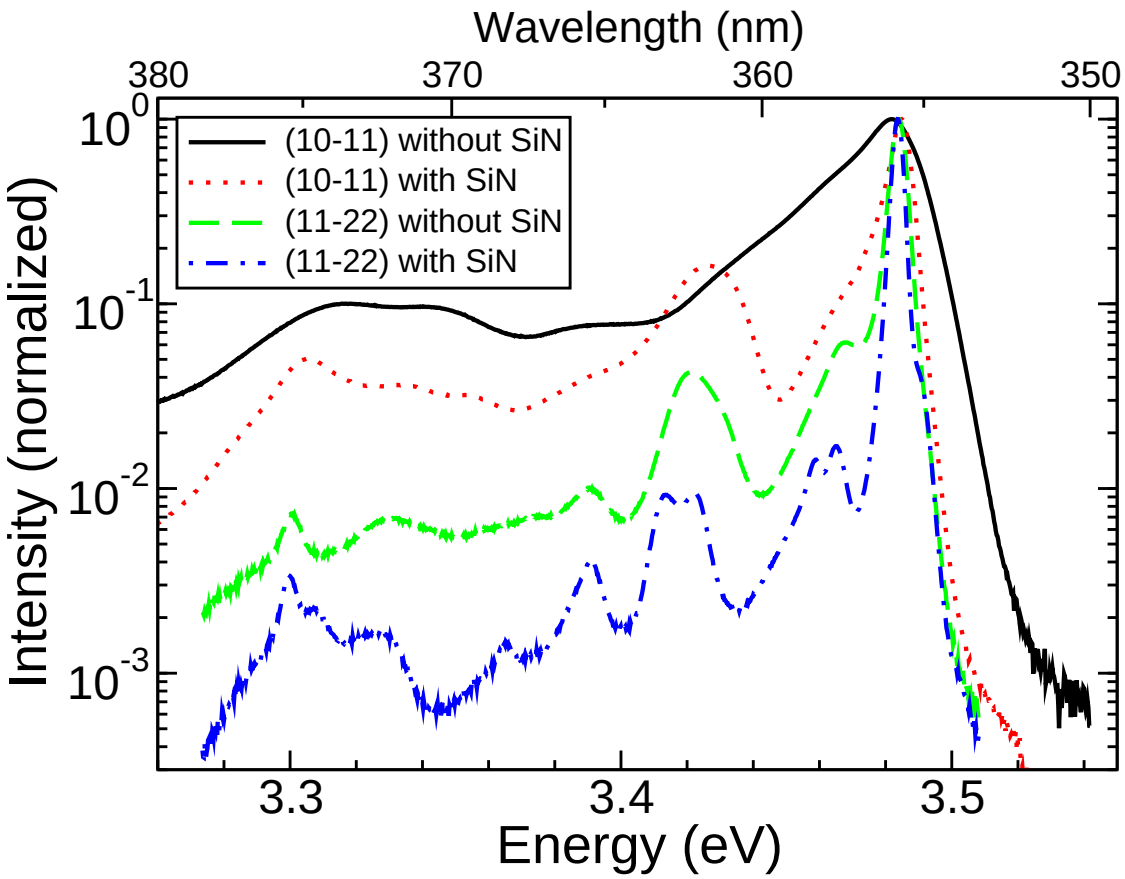

Figure 5. Low-temperature photoluminescence spectra of semipolar GaN layers with $\{10\bar{1}1\}$ and $\{11\bar{2}2\}$ surface grown with and without a SiN nanomask interlayer, as indicated in the figure.

indicating that the chemical surface details also play a major role here, similar to that for the incorporation of In into GaInN [24]. Moreover, we found a strong roughening of the surface for the semipolar GaN:Mg layers, which led to a comparably wide extension of the Mg SIMS profile into the depth of the sample (Fig. 9). Unfortunately, we could not yet measure p-type conductivity on our semipolar layers by simple van der Pauw Hall experiments. This may be partly due to the still low Mg concentration even for the highest doping flows and also due to the above mentioned unintentional n-type conductivity of the buffer layers.

5. Summary

In order to improve our semipolar layers grown out of trenches etched into n-plane and r-plane sapphire wafers, we have optimized the orientation of the nucleation facets by inclining our wafers by a few degrees during the dry-etching procedure. This helps to improve the surface flatness of our $\{11\bar{2}2\}$ samples. Moreover, by integrating a SiN nanomask layer, we could significantly reduce the stacking fault density in our layers. No differences between $\{11\bar{2}2\}$ and c-plane samples could be observed for n-type doping with SiH_4, whereas the Mg incorporation dropped by about a factor of 10 on these semipolar layers as compared to their polar c-plane counter-parts.

6. Acknowledgement

We gratefully acknowledge fruitful discussions with T. Al tahtamouni (home address: Yarmouk University, Irbid, Jordan) and the scientific and technical assistance of B. Neuschl and I. Schwaiger. Parts of this work have been

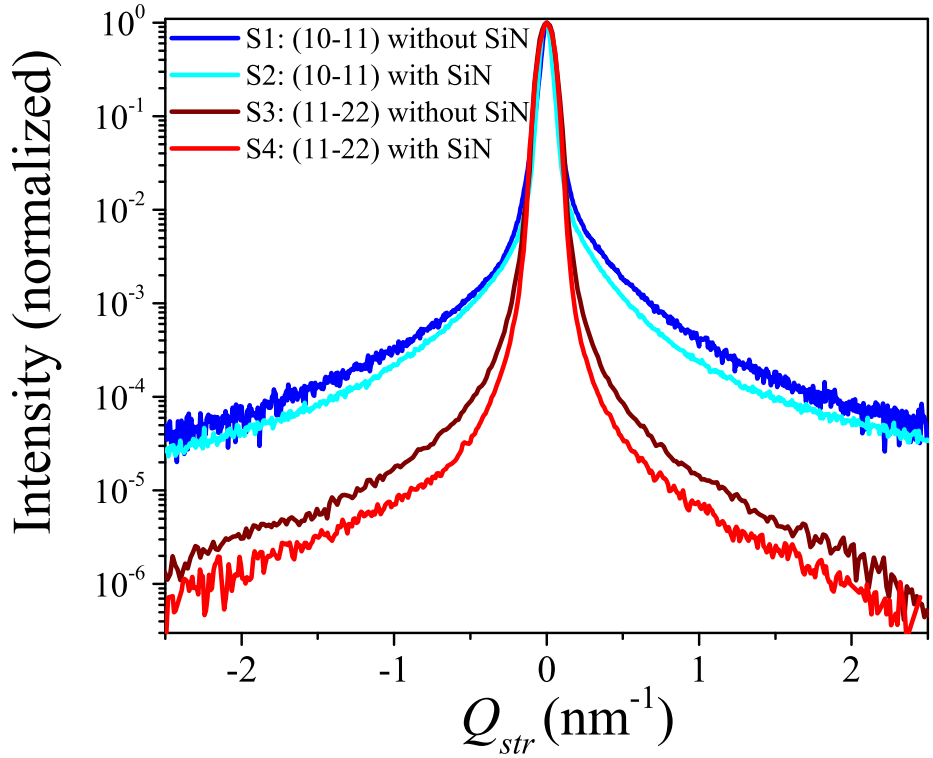

Figure 6. Intensity distribution along stacking fault streaks of semipolar GaN layers with $\{10\bar{1}1\}$ and $\{11\bar{2}2\}$ surface grown with and without a SiN nanomask interlayer, as indicated in Tab. 4.

financially supported by the Deutsche Forschungsgemeinschaft within our transregional research group PolarCoN, by the Bundesministerium für Bildung und Forschung (FKZ 13N9977) and by the EU within the project ALIGHT.

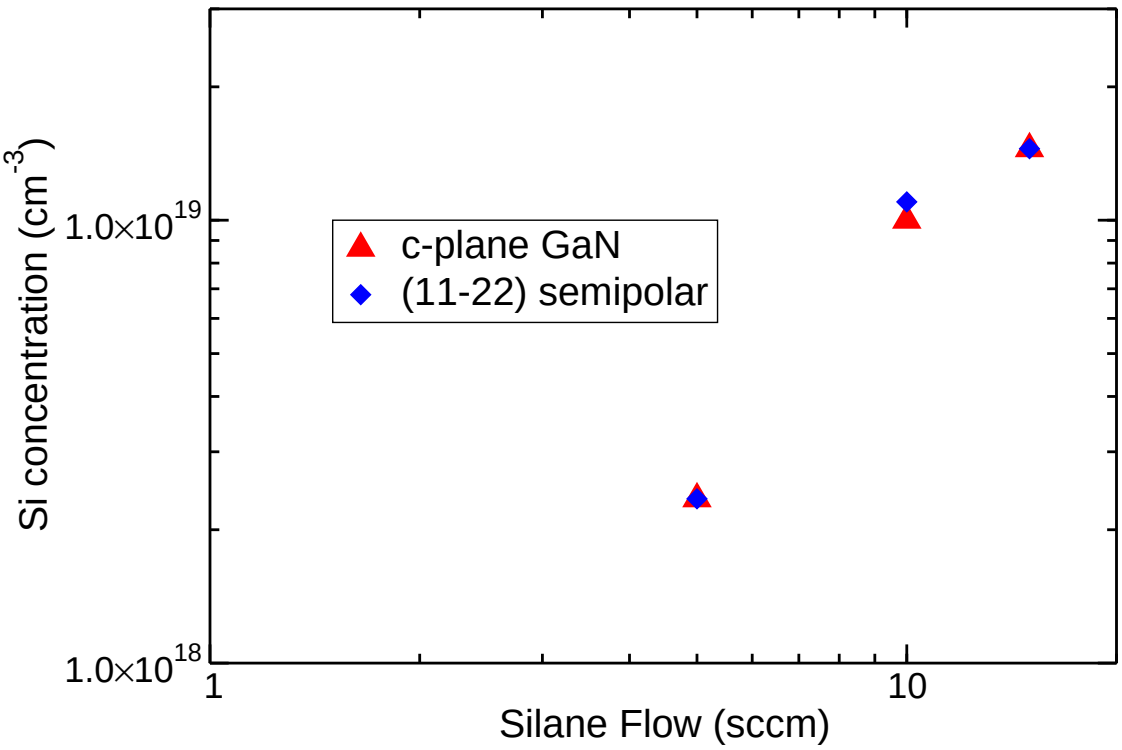

Figure 7. Si concentration measured by SIMS versus SiH_4 precursor flow in c-plane and $\{11\bar{2}2\}$ GaN:Si layers grown side by side in the same runs.

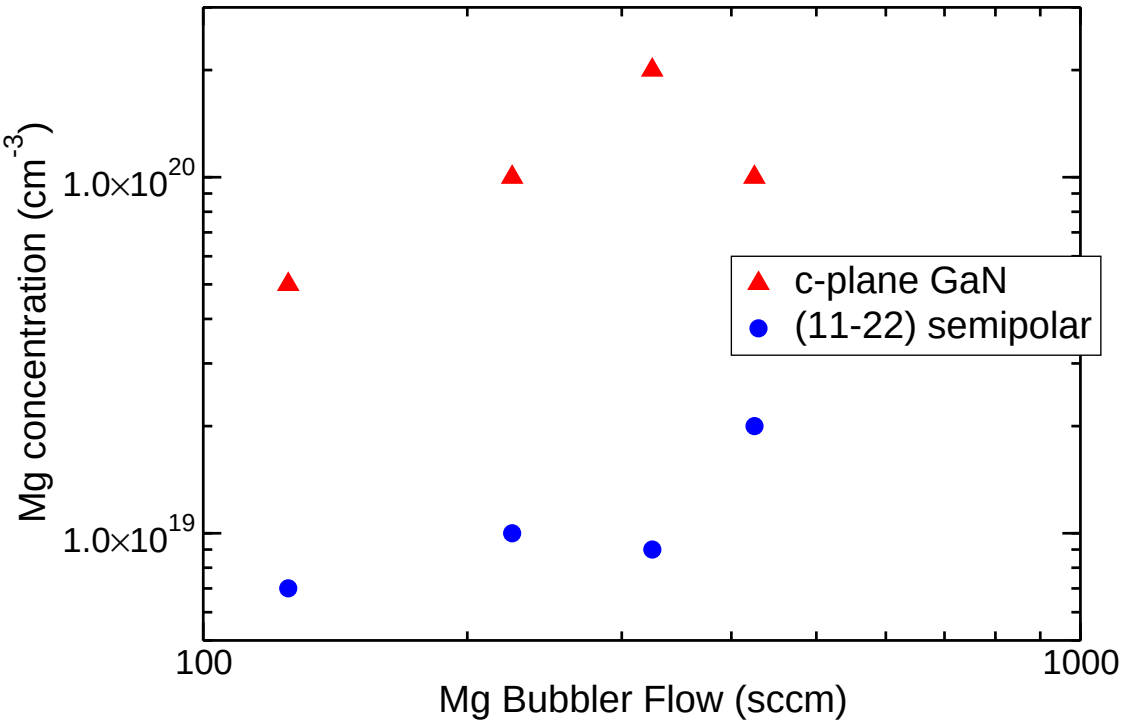

Figure 8. Mg concentration measured by SIMS versus Cp_2Mg precursor flow in c-plane and {11$\bar{2}$2} GaN:Si layers grown side by side in the same runs.

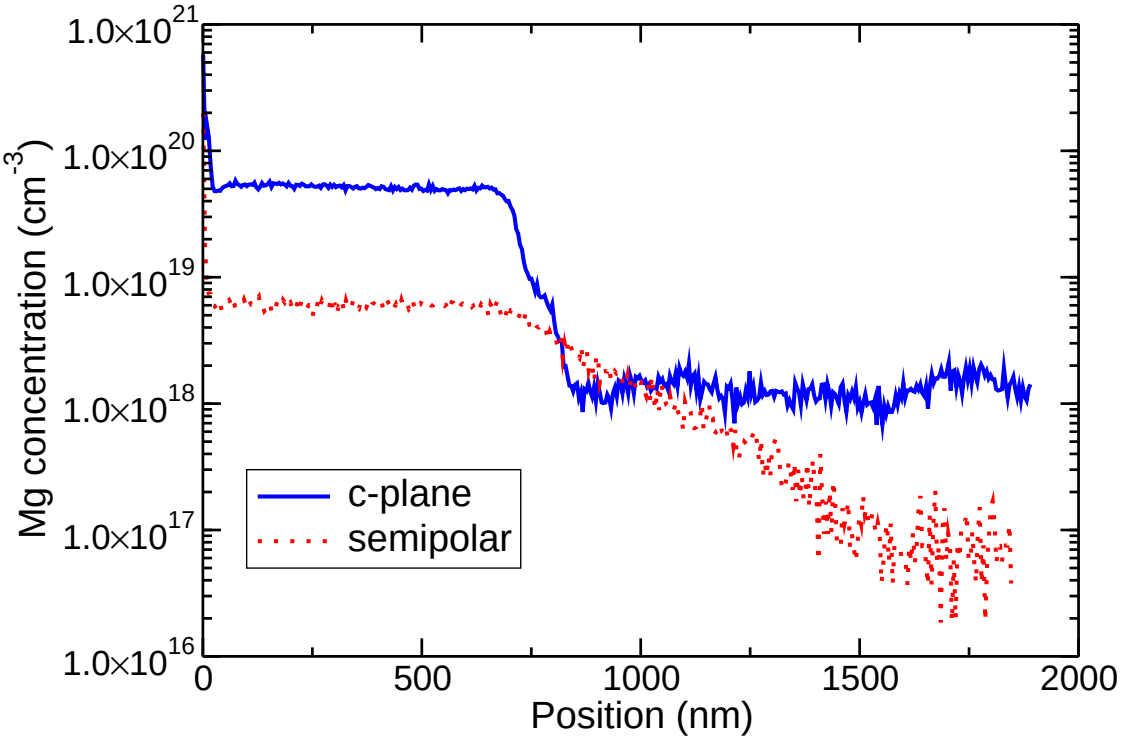

Figure 9. SIMS profiles of a c-plane and {11$\bar{2}$2} semipolar GaN:Mg layer grown side by side in one run.

References

[1] K. Fujito, S. Kubo, I. Fujimura, Development of bulk GaN crystals and nonpolar/semipolar substrates by HVPE, MRS Bulletin 34 (2009) 313–317.

[2] R. Dwilinski, R. Doradzinski, J. Garczynski, L. Sierzputowski, R. Kucharski, M. Zajac, M. Rudzinski, R. Kudrawiec, J. Serafinczuk, W. Strupinski, Recent achievements in AMMONO-bulk method, J. Cryst. Growth 312 (2010) 2499–2502.

[3] R. Kucharski, M. Zajac, R. Doradzinski, J. Garczynski, L. Sierzputowski, R. Kudrawiec, J. Serafinczuk, J. Misiewicz, R. Dwilinski, Structural and Optical Properties of Semipolar GaN Substrates Obtained by Ammonothermal Method, Appl. Phys. Express 3 (2010) 101001–1–3.

[4] F. Scholz, Semipolar GaN grown on foreign substrates: a review, Semicond. Sci. Technol. 27 (2012) 1–15.

[5] Y. Honda, N. Kameshiro, M. Yamaguchi, N. Sawaki, Growth of {1$\bar{1}$01} GaN on a 7-degree off-oriented (001)Si substrate by selective MOVPE, J. Cryst. Growth 242 (2002) 82–86.

[6] N. Okada, H. Oshita, A. Kurisu, K. Tadatomo, Growth Mechanism of Nonpolar and Semipolar GaN Layers from Sapphire Sidewalls on Various Maskless Patterned Sapphire Substrates, Jpn. J. Appl. Phys. 50 (2011) 035602–1–7.

[7] N. Okada, K. Tadatomo, Characterization and growth mechanism of nonpolar and semipolar GaN layers grown on patterned sapphire substrates, Semicond. Sci. Technol. 27 (2012) 024003–1–9.

[8] N. Okada, H. Oshita, K. Yamane, K. Tadatomo, High-quality {20-21} GaN layers on patterned sapphire substrate with wide-terrace, Appl. Phys. Lett. 99 (2012) 242103–1–3.

[9] N. Okada, K. Uchida, S. Miyoshi, K. Tadatomo, Green light-emitting diodes fabricated on semipolar (1122) GaN on r-plane patterned sapphire substrate, Phys. Status Solidi A 209 (2012) 469–472.

[10] P. Vennéguès, B. Beaumont, S. Haffouz, M. Vaille, P. Gibart, Influence of in situ sapphire surface preparation and carrier gas on the growth mode of GaN in MOVPE, J. Cryst. Growth 187 (1998) 167–177.

[11] S. Sakai, T. Wang, Y. Morishima, Y. Naoi, A new method of reducing dislocation density in GaN layer grown on sapphire substrate by MOVPE, J. Cryst. Growth 221 (2000) 334–337.

[12] J. Hertkorn, F. Lipski, P. Brückner, T. Wunderer, S. B. Thapa, F. Scholz, A. Chuvilin, U. Kaiser, M. Beer, J. Zweck, Process optimization for the effective reduction of threading dislocations in MOVPE grown GaN using in situ deposited SiN_x masks, J. Cryst. Growth 310 (2008) 4867–4870.

[13] B. Kuhn, F. Scholz, An Oxygen Doped Nucleation Layer for the Growth of High Optical Quality GaN on Sapphire, Phys. Status Solidi A 188 (2001) 629–633.

[14] J. Hertkorn, P. Brückner, S. B. Thapa, T. Wunderer, F. Scholz, M. Feneberg, K. Thonke, R. Sauer, M. Beer, J. Zweck, Optimization of nucleation and buffer layer growth for improved GaN quality, J. Cryst. Growth 308 (2007) 30–36.

[15] S. Lazarev, S. Bauer, K. Forghani, M. Barchuk, F. Scholz, T. Baumbach, High resolution synchroton X-ray studies of phase separation phenomena and the scaling law for the threading dislocation densities reduction in high quality AlGaN heterostructure, J. Cryst. Growth 370 (2013) 51–56.

[16] S. Lazarev, M. Barchuk, S. Bauer, K. Forghani, V. Hol, F. Scholz, T. Baumbach, Study of threading dislocation density reduction in AlGaN epilayers by Monte Carlo simulation of high-resolution reciprocal-space maps of a two-layer system, Journal of Applied Crystallography 46 (2013) 120–127.

[17] S. Lazarev, S. Bauer, T. Meisch, M. Bauer, I. Tischer, M. Barchuk, K. Thonke, T. Baumbach, V. Holy, F. Scholz, 3D Reciprocal space mapping of diffuse scattering for the study of stacking faults in semipolar (11$\bar{2}$2) GaN layers grown from the sidewall of an r-patterned sapphire substrate, J. Appl. Cryst. 46 (2013) 1425–1433.

[18] M. Caliebe, T. Meisch, B. Neuschl, S. Bauer, J. Helbing, D. Beck, S. Schörner, K. Thonke, M. Klein, D. Heinz, F. Scholz, Improvements of MOVPE grown (11$\bar{2}$2) oriented GaN on pre-structured sapphire substrates using a SiN_x interlayer and HVPE overgrowth, Phys. Status Solidi C 11 (2014) 525–529.

[19] D. Min, G. Yoo, Y. Ryu, S. Moon, K. Lee, O. Nam, Improvement of crystal quality and optical property in (11-22) semipolar InGaN/GaN light emitting diodes grown on hemi-spherically patterned SiO_2 mask, J. Ceramic Processing Res. 14 (2013) 521–524.

[20] N. Kriouche, P. Vennéguès, M. Nemoz, G. Nataf, P. deMierry, Stacking faults blocking process in (11$\bar{2}$2) semipolar GaN growth on sapphire using asymmetric lateral epitaxy, J. Cryst. Growth 312 (2010) 2625–2630.

[21] T. Zhu, D. Sutherland, T. J. Badcock, R. Hao, M. A. Moram, P. Dawson, M. J. Kappers, R. A. Oliver, Defect Reduction in Semi-Polar (11$\bar{2}$2) Gallium Nitride Grown Using Epitaxial Lateral Overgrowth, Jpn. J. Appl. Phys. 52 (2013) 08JB01–1–5.

[22] S. Schwaiger, S. Metzner, T. Wunderer, I. Argut, J. Thalmair, F. Lipski, M. Wieneke, J. Blaesing, F. Bertram, J. Zweck, A. Krost, J. Christen, F. Scholz, Growth and coalescence behaviour of semipolar {11$\bar{2}$2} GaN on pre-strucured r-plane sapphire substrates, Phys. Status Solidi B 248 (2011) 588–593.

[23] S. C. Cruz, S. Keller, T. E. Mates, U. K. Mishra, S. P. DenBaars, Crystallographic orientation dependence of dopant and impurity incorporation in GaN films grown by metalorganic chemical vapor deposition, J. Cryst. Growth 311 (2009) 3817–3823.

[24] J. E. Northrup, GaN and InGaN (11$\underline{2}$2) surfaces: Group-III adlayers and indium incorporation, Appl. Phys. Lett. 95 (2009) 113107–1–3.